

The case of the two-period polar BY Cam (H0538+608) *

M. Mouchet^{1,2}, J.M. Bonnet-Bidaud³, N.N. Somov⁴, T.A. Somova⁴

¹Observatoire de Paris, DAEC, Unité associée au CNRS et à l'Université Paris 7-Denis Diderot, F-92195 Meudon Cedex, France

²Université Denis Diderot, Place Jussieu, F-75005 Paris Cedex, France

³Service d'Astrophysique, CE Saclay, CEA/DSM/DAPNIA/SAP, F-91191 Gif sur Yvette Cedex, France

⁴Special Astrophysical Observatory of the Russian Academy of Sciences, Nizhnij Arkhyz 357147, Russia

Received: 1996 November 26; accepted: 1997 February 3

Abstract. We present the results of fast temporal optical spectroscopy and photometry of the AM Her type system BY Cam obtained in February 1990 and March 1991. Emission line profiles show a complex structure and are strongly variable. The radial velocity studies of a sharp component detected in Balmer lines in March confirms the non-synchronism of the system. Different possible emitting regions are discussed to explain the characteristics of the multiple line components. It is shown from a computation of the line velocities and widths that the 'horizontal' stream cannot explain the lines of intermediate widths observed in this system. A critical review of the different estimations of the periods found in BY Cam is presented. Additional periods are revealed from a re-analysis of previous optical polarimetric and UV spectroscopic data. We show that because of the slight asynchronism between the white dwarf rotation and the orbital period, significant changes in the accretion geometry introduce a bias in the period determination depending on the length of the observations. Large phase variations are shown to exist which are well reproduced by a phase-drift model in which a magnetic dipole rotates in the orbital frame with a period of 14.5 ± 1.5 days.

Key words: Accretion, accretion column – stars: individual BY Cam – binaries: Cataclysmic Variables, Polars – Optical: Spectroscopy, Photometry

1. Introduction

Polars (AM Her type systems) are cataclysmic binaries in which a magnetic white dwarf accretes matter from a red dwarf star filling its Roche lobe. The accretion occurs along the magnetic field lines down to the magnetic poles of the white dwarf. The X-rays and the optical polarized flux, both originating close to the surface of the white dwarf are modulated at the orbital period which proves the synchronism of the white dwarf rotation with the orbital motion. A comprehensive review of these objects has been done by Cropper (1990).

In the case of BY Cam, the situation concerning the different periods in the system is not clear. The X-ray source H0538+608 (BY Cam) has been identified as a polar by Remillard et al.(1986), on the basis of the detection of a circularly polarized optical flux. This source shows two brightness states (Szkody et al. 1990), such a behaviour being shared by most polars. However this object is atypical by several aspects. In the UV it reveals an abnormal emission line spectrum with an enhanced NV line and a weak CIV line (Bonnet-Bidaud and Mouchet 1987). This could be linked to the chemical composition of a secondary whose outer layers have been lost during the evolution of the system (Mouchet et al. 1991). This is also reminiscent of what is found in some novae, suggesting a possible unnoticed nova-like event (Bonnet-Bidaud and Mouchet 1987). However no nova outburst is recorded in archive plates (Silber et al. 1992 (hereafter SBIOR)). Noteworthy, X-ray spectra of BY Cam obtained with the BBXRT experiment revealed an oxygen absorption edge near 0.6 keV, which intensity either requires an overabundance of oxygen or partially ionized material (Kallman et al. 1993).

Contemporaneous X-ray and optical observations (Ishida et al. 1991, SBIOR) have revealed the presence of two very close periods around 3.3h, suggesting the asynchronism of the system (SBIOR). This was the second polar sharing this peculiarity: the first one being V1500 Cyg,

Send offprint requests to: M. Mouchet (mouchet@obspm.fr)

* Based on observations from State Research Center Special Astrophysical Observatory of Russian Academy of Sciences, Russia.

Table 1. Log of the photometric and spectroscopic observations

date	Photometry				V mag.	Spectroscopy			
	start (UT)	end (UT)	phase start-end	total exp.		start (UT)	end (UT)	phase start-end	total exp.
25 Feb. 90	17:40	20:46	0.22-1.15	3h06m	14.6	17:39	19:04	0.22-0.61	2h15m
						19:51	20:41	0.90-1.11	
10 March 91	16:44	21:10	0.67-2.01	3h26m	15-15.6	16:32	17:42	0.63-0.93	4h14m
						17:49	18:49	1.02-1.27	
						18:57	20:01	1.36-1.62	
						20:05	21:06	1.71-1.96	
12 March 91	16:43	20:13	0.12-1.17	3h30m	14.2-14.9	16:39	17:39	0.11-0.32	3h29m
						17:44	18:16	0.44-0.53	
						18:21	19:33	0.63-0.92	
						19:38	20:23	1.01-1.18	

a nova which is expected to become synchronous again in less than 200 years (Schmidt and Stockman 1991, Katz 1991). A third one, RX J1940.1-1025, has been added recently, but contrary to both previous ones, the spin period is slightly longer than the orbital period (Friedrich et al. 1996). From a compilation of previous optical polarimetric and photometric measurements of BY Cam, combined with new observations, Pirola et al. (1994) obtained a new determination of the shortest period (3.3308h) which differs significantly from the original determination (Mason et al. 1989, hereafter MLS). The presence of two close periods in this system led to search for a longer period of the order of fourteen days which would be the beat period. A large set of photometric data collected over a period of 66 days, seem to reveal a period of seven days (Silber 1995), but a beat period of 14 days has also been suggested by Mason et al. (1995a,b).

Recently, time-resolved UV spectroscopy revealed a modulation of the line fluxes and of the radial velocities with the longest period identified as the orbital one (Zucker et al. 1995), implying an origin far from the accretion column, contrary to the common idea that the high ionization UV resonance lines are formed close to the white dwarf. In the optical emission lines are very complex and can show up to four components (MLS).

In this paper we present an analysis of high temporal resolution spectroscopic and photometric optical data obtained at three different dates. Partial results have been presented by Bonnet-Bidaud et al. (1992). The optical emission lines, composed of components arising from different regions, are good tools to constrain the different periods present in this system and to trace the geometry of the accreting flow. The optical results are compared to the UV spectroscopic results. A critical review of the different period determinations is also presented in Sec-

tion 5 and their interpretation is discussed in Section 6 in terms of phase-drifts introduced by an asynchronous rotating magnetosphere.

2. Observations

Spectroscopic and photometric data were obtained simultaneously at the AS SAO 6m telescope in Zelenchuk (Russia) in February 1990 and March 1991. The observations were performed using the SP-124 spectrograph and the NEF photometer at the Nasmyth secondary focus of the 6 meter Bolshoi Azimuthal Telescope (Ioannisianni et al. 1982, Vikuliev et al. 1991). The spectrograph was equipped with a 1200 lines/mm grating. A television scanner with two lines of 1024 channels was used to record the sky and source spectra simultaneously in a photon-counting mode (see Somova et al. (1982), Drabek et al. 1986, Afanasiev et al. 1991, for a detailed description of the instrumentation). The intrinsic temporal resolution is 0.033 s. The wavelength range was 3900-4920Å, 4030-5050Å and 3950-4970Å respectively in Feb. 1990, on March 10 and March 12 1991. A wavelength calibration has been applied using a He-Ar-Ne lamp. The aperture is a circular slit which diameter was chosen between 2 and 3", according to the seeing. The corresponding spectral resolution is $\sim 2.5\text{\AA}$. The sky spectrum has been subtracted but no flux calibration has been applied. The log of the observations is reported in Table 1. Photometric data were obtained simultaneously with the spectroscopic data by splitting the light beam, with about 50% of the light being sent into a 12" aperture one-channel fast photometer. Continuous Johnson B data were recorded with a 0.1s resolution. UBVR were also acquired in one or two occasions during each observation and have been used to compute the optical magnitude of the source using star F from 3C147 field (Neizvestny 1995) as a reference star. The

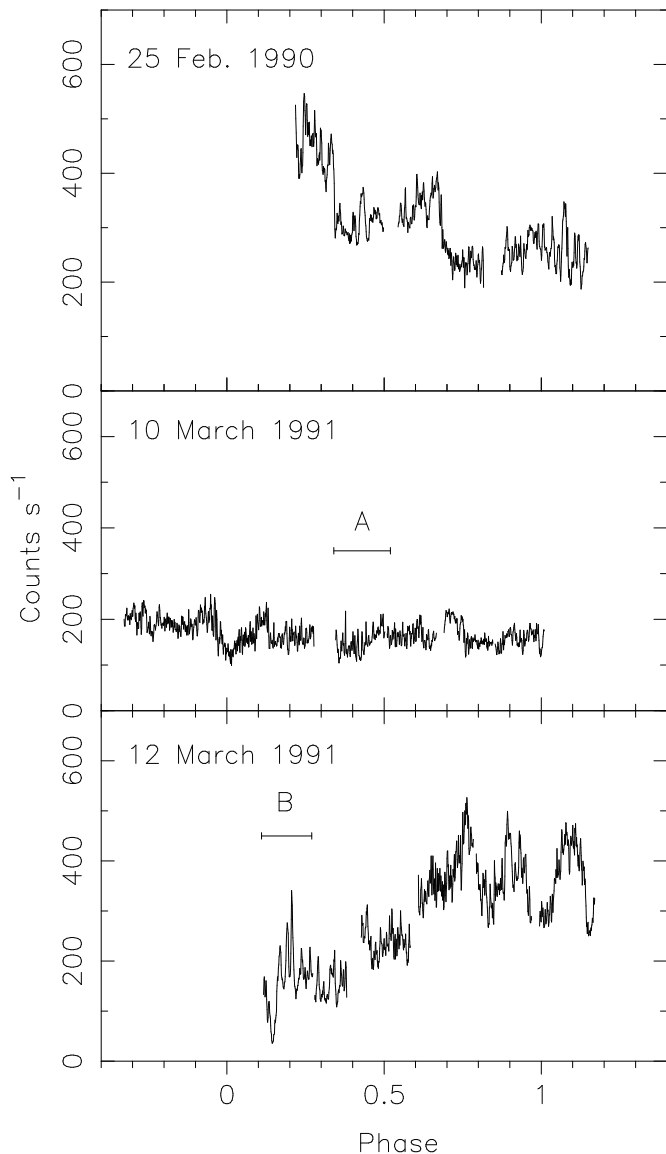


Fig. 1. The air-mass and sky-corrected optical B light curves of BY Cam for the three observing dates. The phase is computed with the trial ephemeris of Mason et al. (1989). The regions marked A and B are enlarged in Figure 2. Note the different brightness levels and the strong variability on Feb. 25 1990 and March 12 1991.

V magnitude values, reported in Table 1, show the source to be in a high state during the three observations, distinct from the low state observed by Szkody et al. (1990) in January 1989. When two measurements have been done during the same night, their different values are consistent with the amplitude of the light curve (Remillard et al. 1986, SBIOR).

Throughout this paper, heliocentric phases refer to the ephemeris given by MLS that is used as a comparison ephemeris. Given the uncertainty in the determina-

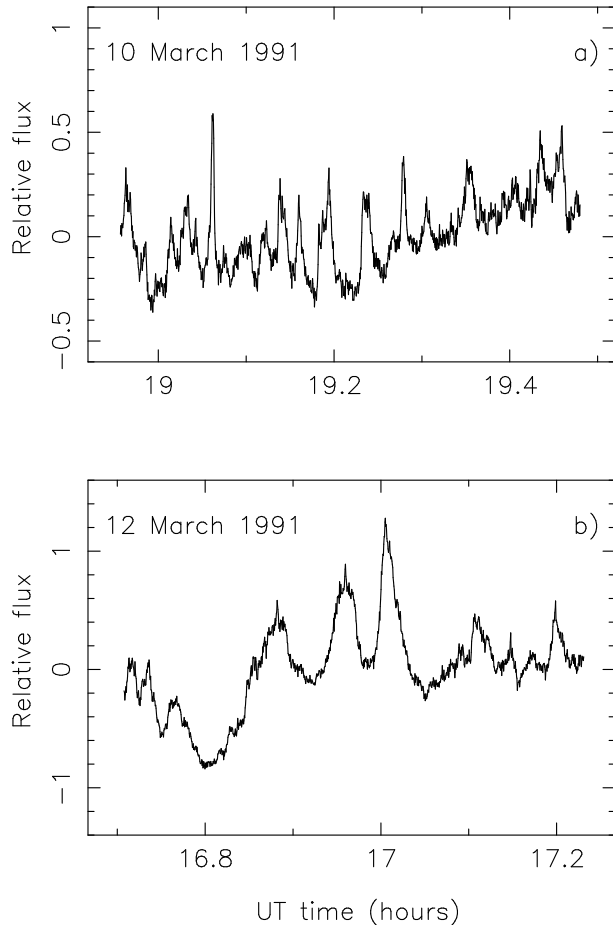


Fig. 2. Enlargements of the optical B light curves of BY Cam on March 10 (a) and on March 12 (b) for an illustration of the strong variability. The plotted parts are marked A and B in Fig.1. The temporal resolution is 1.6 s for both curves. The vertical scale is the deviation in % from the mean flux value of the corresponding part of the light curve.

tion of the different periods of the system, the accuracy given in this ephemeris is purely formal and the period (3.322171 ± 0.000017 h) is used here only as a trial period to facilitate the comparison with other works (see par. 5.1).

3. Photometry

In Figure 1 we show the B light curves obtained simultaneously with the spectroscopic data, at a temporal resolution of 12.8 s for the three observing dates. They reveal two levels of activity. On February 25 1990 and on March 12 1991 the large amplitude of the modulation is reminiscent of the flaring states observed in the optical as well as in the X-rays by Ishida et al. (1991) and SBIOR, while on March 10, the light curve shows a lower intensity which indicates a level closer to a pulsing state (Ishida et al.

1991, SBIOR). For both February 25 and March 12 observations, the lowest levels of the light curves which occur at the end and at the beginning of the observations respectively, are consistent with the level detected on March 10. The higher fluxes in 25 Feb 1990 and 12 March 1991 compared to March 10 suggest an additional source of light. During a flaring state, SBIOR have reported a one-peaked periodic light curve, which exhibits an increase by a factor ~ 2 between the minimum and the maximum. The Feb. and March 12 curves also exhibit a total variation by a factor 2-2.5, but their strong variability excludes a regular quasi-sinusoidal shape. However, Silber (1995) reports flaring state light curves which also depart from a regular shape.

The March 10 light curve varies in amplitude by a lower factor of 1.5, quite consistent with the pulsing state light curves shown in SBIOR. There is no clear indication of the presence of two maxima, while these bumps are usually seen in the low-level optical curves with possible unequal intensities and separated by a variable phase extension (SBIOR, Silber 1995).

Apart from the large amplitude main modulation, these optical light curves show shorter timescale variability. We note a significant (~ 5 min.) dip seen near phase 0.1 on March 12. In Figure 2, are reported two blow-ups of March 10 and March 12 light curves exhibiting strong flaring on a typical timescale of 1-2 minutes on March 10 and of 3-5 minutes on March 12. The FFT power spectrum analysis of the data does not show significant power excess at these periods indicating that these oscillations are not coherent. On March 12, quasi-periodic oscillations of the order of 30 minutes are visible in the second part of the light curve (Fig.1), similar to what reported previously by SBIOR.

4. Spectroscopy

4.1. Description of the line profiles

Spectra averaged over the full observation have been produced for the three dates. They are similar to previously published spectra, exhibiting the usual strong Balmer and helium lines (Remillard et al. 1986, MLS). In order to study the orbital and rotational modulation of the line profiles, the spectra have been co-added with a 500s resolution which is the best compromise between a high temporal resolution and a good signal-to-noise ratio. This results in 16, 29 and 22 spectra respectively on 1990 Feb. 25, 1991 March 10 and March 12. The spectra reveal the presence of several variable components in both Balmer and He lines. In Fig. 3 the HeII and H_β profiles normalized to the continuum are shown for the three epochs in order of increasing phase from bottom to top. Large variability with phase at a given epoch as well as strong changes be-

tween the three observations are clearly seen. Remarkably, the HeII profile differs from the H_β profile in most spectra. The most complex profiles appear in Feb. 90 in both Balmer and HeII line while in 1991, they are restricted to the Balmer components only, the HeII line showing a much more regular phase variation.

4.2. Radial velocity results

The very complex and variable line profiles observed in BY Cam make the radial velocity (RV) analysis very difficult. In addition, blends with close weaker lines might occur (f.i. HeI 4713Å in the red wing of HeII 4686Å) and affect the measurements. To isolate the different components of the complex emission lines, the profiles have been fitted with the sum of two or three gaussians of variable widths, intensities and positions, using the program SPECTRE developed by D. Pelat at Meudon Observatory. In this program free parameters are the width, intensity and centre of the gaussians as well as the adjacent continuum which is fitted with a polynomial of degree one.

The results of the gaussian fits of the HeII 4686Å and H_β profiles have been used to derive the velocity curves of the different components. The measured radial velocities for HeII and for H_β were fitted with a sinusoid $V(\phi) = \gamma + K \sin 2\pi(\phi - \phi_0)$, ϕ being the phase computed from the MLS ephemeris. The best fit parameters are reported in Table 2 where the error bars correspond to a 1σ deviation. The uncertainties given in Table 2 do not take into account possible systematic uncertainties in the absolute calibration. The errors in the absolute γ -velocity are therefore underestimated.

Multiple components are clearly present and the deconvolution may not be unique in some cases. The FWHM of the different components are given in Table 2, corrected for the instrumental response. In February 90, the HeII line is wide and exhibits a complex profile: in addition to a narrow width (FWHM ~ 200 km s^{-1}) component and a broad (FWHM ~ 1140 km s^{-1}) one, a very blue high velocity shoulder is detectable mostly between phases 0.4 and 0.6. The RV measurements of the narrow and broad components can be satisfactorily fitted with a sinusoidal curve, while the measurements of the blue high velocity component are more scattered (Fig. 4a,b,c). The narrow and broad components appear in phase but with different amplitudes. The high velocity component lags the two others by 0.4 in phase. It appears not to be similar to the very high velocity component detected by MLS. Indeed there is no clear indication of a red counterpart at opposite phases and the observed modulation is not compatible with an amplitude as large as ~ 800 km s^{-1} found by MLS. Its low amplitude and its large negative γ -velocity seem to favour an origin close to the white dwarf, such as a Zeeman component which has been already proposed by

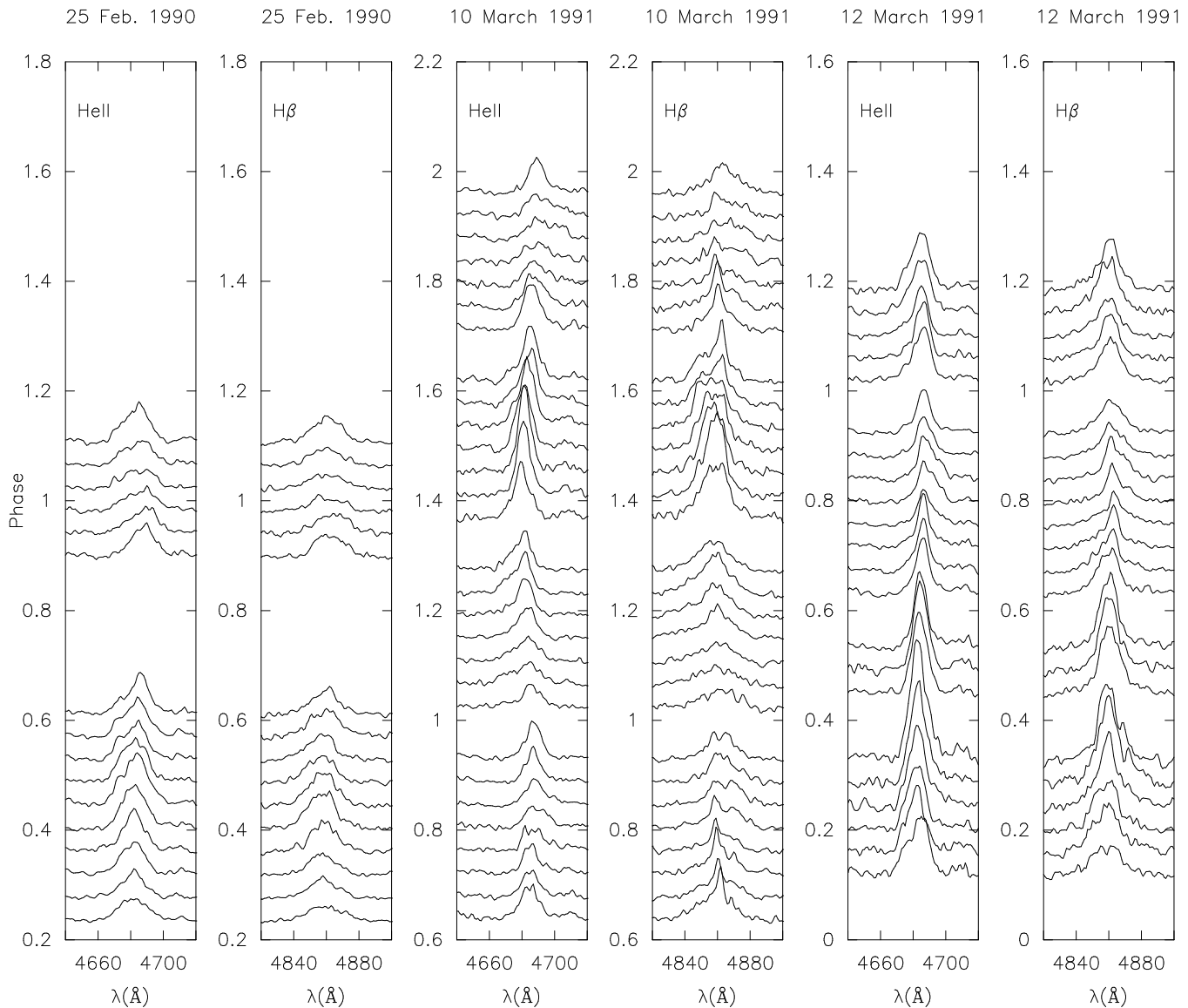


Fig. 3. HeII and H_{β} normalized profiles at the same scale, on February 25 1990, on March 10 1991 and on March 12 1991. Phase is increasing from bottom to top as shown on the Y-axis.

McCarthy et al. (1986) to explain the stationary high velocity narrow component found in the HeII lines of QQ Vul. At the same epoch, the Balmer lines show more complex profiles than the HeII (Fig. 3) and sinusoidal fits cannot be quoted unambiguously.

In March 1991, the Balmer and HeII lines are strongly variable. The HeII line essentially exhibits two components, one broad and one of intermediate width ($\text{FWHM} \sim 400 \text{ km s}^{-1}$) with no evidence of the narrower ($\text{FWHM} \leq 200 \text{ km s}^{-1}$) component seen in Feb. 90. On March 10, radial velocities of the intermediate width HeII component are satisfactorily described with a sinusoidal fit, while on March 12, this component is definitely present but its RV curve departs from a sinusoidal curve, being

quasi-stationary between phase 0.6-1.05. For both dates, the radial velocities of the broad component in HeII have been fitted, though on March 12 they show a significant distortion around phases 0.2-0.4 (see Fig. 4f). The resulting amplitude is lower by 25% on March 12 than on March 10 and the radial velocities on March 10 lag the ones on March 12 by 0.11 in phase (Fig. 4d,f).

The RV measurements of the broad component in H_{β} also strongly depart from a well-defined sinusoidal curve, particularly on March 12 (Fig. 4e,g). The distortions present in these RV curves are characterized by a shoulder present at phases 0.2-0.5, at the two dates, being markedly pronounced on March 12. It is reminiscent of what has been seen in the flaring state data presented by SBIOR. The

Table 2. Averaged deconvolved FWHM and radial velocity sinusoidal parameters of the HeII and H_β line components

date	line	component	FWHM km s ⁻¹	γ -vel* km s ⁻¹	K amplitude km s ⁻¹	ϕ_0
25 Feb. 90	HeII	narrow	200±90	49±16	265±24	0.608±0.013
		broad	1135±135	-50±17	160±24	0.591±0.022
		high velocity	405±70	-818±15	158±28	0.983±0.018
10 March 91	H_β	narrow	165±35	18±35	230±23	0.138±0.025
	HeII	intermediate width	395±100	-105±10	172±14	0.648±0.012
		broad	1060±260	-109±10	357±13	0.563±0.007
12 March 91	H_β	narrow	250±45	-93±51	214±49	0.389±0.0027
	HeII	broad	1110±220	-34±10	250±16	0.449±0.009

* These values should be regarded with caution due to the large uncertainty of the absolute wavelength calibration

RV curves cannot be described by a sinusoidal curve in this case. It may indicate either the presence of an additional redder component or a partial eclipse of the broad component at these phases. Noteworthy, similar deviations have been reported for V1500 Cyg by Kaluzny and Chlebowski (1988) who have attributed them to the contribution of a second accreting column.

At the difference of the HeII line, the H_β and H_γ profiles show the presence of a narrow (FWHM~150-250 km s⁻¹) component. The peak is clearly observed around phases 0.5 to 0.9 and repeatable from cycle to cycle. The velocity curve of this component is shown in Figure 5. This component being clearly detectable at specific phases only, the corresponding fits are thus less constrained. The amplitude are similar but an obvious lag in phase is observed for the two observations separated by two days when data are folded with the trial period (3.322171h) derived by MLS.

This phase difference (0.251 ± 0.037) is consistent with an orbital period ($1.8 \pm 0.3\%$) longer than the trial period. The best period derived from our narrow-line observations only will be (3.3817 ± 0.0085 h). This is slightly longer, but consistent within the error bars, with the value derived by SBIOR from the H_α narrow line velocity. This provides an independent confirmation that the period deduced from the narrow-line measurements, usually associated with the orbital period, is significantly longer than the period derived from polarimetry. We investigate more about the nature of the two periods in Section 5.

A broad component is obviously present in all data, but its characteristics and its corresponding sinusoidal parameters can only be safely derived for the HeII compo-

nent. Its width and K amplitude are typical of those measured in other polars and the origin of this component is attributed to regions down to the accretion column (Ferrario et al. 1989, Mouchet 1993b). In 1991 its relative phasing with respect to the narrow H_β component is 0.42 and 0.06 on March 10 and March 12 respectively, confirming the asynchronism of the system.

5. Discussion

5.1. Emission lines from the horizontal stream

The true location of the emission line regions in polars is still a subject of discussion. Two main components are usually considered: a broad line associated with the accretion column and linked to the rotation of the white dwarf and a narrow line associated with the heated face of the secondary, linked to the orbital period. In the case of the complex multi-component profiles observed in BY Cam, the situation is more intricate and several other regions may contribute to build the resulting profile. In an effort to reproduce the non-standard observed components, we have investigated a region which has not been yet considered in detail, i.e. the horizontal stream of matter that links the secondary to the accretion capture region, roughly defined by the so-called magnetic capture radius.

Before being captured by the magnetic field lines, material forms a stream of matter in the orbital plane (Liebert & Stockman 1985) (referred below as the horizontal stream, as opposed to the accretion column which refers to the out-of-plane part of the accreting flow). This stream has been suggested as a possible contributor to

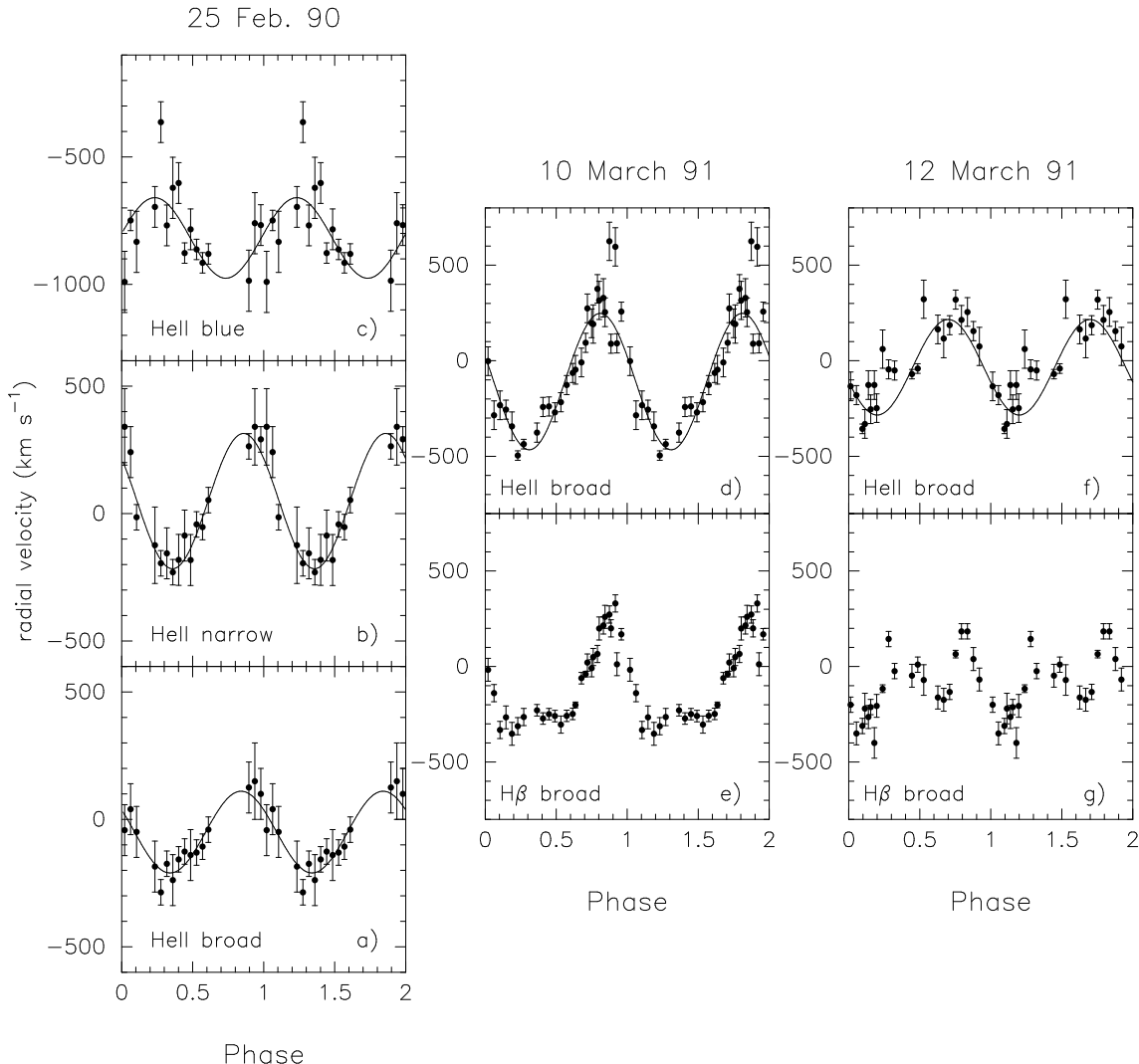


Fig. 4. Radial velocities against phase computed using Mason’s ephemeris for the different components detected in the line profiles. Left: for the three components detected in the HeII profile on February 25 1990: a) broad component; b) narrow component; c) blue high velocity component. Middle: for the broad component of the HeII (d) and $H\beta$ (e) profiles on March 10. Right: for the broad component of HeII (f) and $H\beta$ (g) on March 12. Best sinusoidal fits are reported (see parameters in Table 2), except for f and g which have not been fitted since they markedly depart from a sinusoidal curve (see text).

the emission line profiles (Mukai 1988, Mouchet 1993a). The profile characteristics of a component formed in the horizontal stream mainly depend on the position and on the extension of the emitting region. We have simulated the emission from the stream, assuming that its path is given by the ballistic trajectory as computed by Lubow & Shu (1975). This stream is supposed to extend down to a distance r_c at the capture point where the ram pressure in the horizontal stream equals the magnetic pressure (see more details in Bonnet-Bidaud et al. 1996). To evaluate r_c , we have supposed that the lateral extension of the stream is constant, being taken equal to 10^9 cm (Lubow & Shu 1975, Mukai 1988). We assume a $1 M_\odot$ white dwarf

mass, a typical accretion rate of 10^{-16} g s $^{-1}$, and a dipole geometry with a typical polar field of 40 MG consistent with the evaluations by Cropper et al.(1989) and Pirola et al.(1994). Note however that Mason et al.(1995b) suggest evidence of a more complex field geometry with accretion onto a multipole magnetic field. For the line profile simulation, free parameters are the mean location of the emitting region, its extension and the emissivity of each part of the region together with the mass of the white dwarf, the inclination angle and the orbital period. Since no detailed physical model is available at present to give the exact emissivity in the lines, we made the simple assumption of an emissivity through the emitting re-

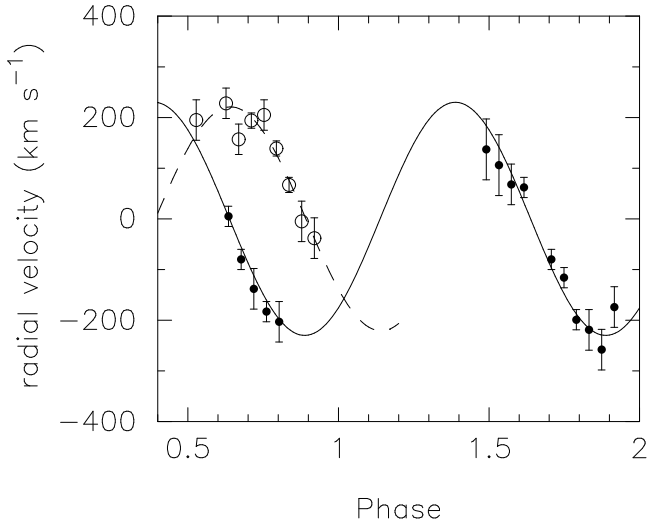


Fig. 5. Radial velocities versus phase computed using Mason’s ephemeris for two observations separated by two days of the narrow component of $H\beta$ on March 10 (filled circles) and on March 12 (open circles). Data are not repeated, March 10 covering more than 1.3 cycle. For both dates, the data have been offset from the γ -velocity value derived from the fit. The corresponding best sinusoidal fits are shown. Note the significant phase lag which can be accounted for by a revised period of $P=(3.3817 \pm 0.0085\text{h})$.

gion defined as a gaussian law with a width equal to the extension. The emissivity is taken null outside the chosen portion of the stream. The computed phase-resolved profiles have been convolved with a spectral resolution of 1 \AA . As illustration, Figure 6 shows different resulting profiles computed at twenty equally spaced orbital phases for two selected emitting regions, each defined by their projection onto the line of centres and expressed in units of the distance X_L between the white dwarf and the inner Lagrangian point. Fig. 6a corresponds to a stream extension between 0.3 to 0.5 times X_L , and Fig. 6b to a region far from the white dwarf, between 0.7 and 0.9 times this distance. An inclination angle of 70° has been assumed. These profiles clearly show a two-peaked orbitally modulated width (Fig. 6c). We stress that the lines produced in the stream would therefore in general be strongly variable in shape and width, appearing alternatively narrow and broad within the same cycle. Such lines would thus be difficult to extract by the standard two-component analysis. However such high temporal and spectral resolution measurements are difficult to derive from most data. Therefore only the phase-averaged full widths at half maximum expected from different zones of the stream have been compared to the data. In Figure 7 these intrinsic widths are reported against the amplitudes K of the RV curves of the lines emitted by seven regions of variable positions (a) and extensions (b). The inclination angle increases along the

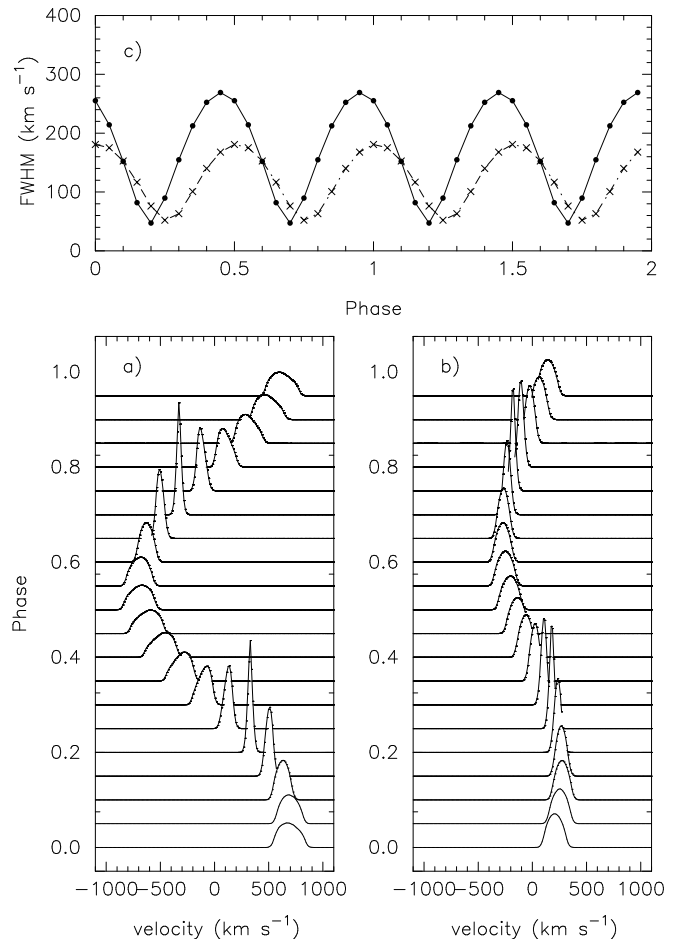


Fig. 6. Simulated profiles for emission lines arising in the ‘horizontal’ stream, for an inclination angle of 70° and a white dwarf mass of $1M_\odot$. A resolution of 1 \AA has been assumed. Left (a): extension of the emitting region from 0.3 to 0.5 times the projected distance between the white dwarf centre and the inner Lagrangian point. Right (b): same as (a) for a smaller extension from 0.7 to 0.9 times this distance. Upper panel (c): the FWHM versus orbital phase for the two sets of simulated profiles (full line: case a) ; dotted line: case b)). The origin of the phase is taken at the inferior conjunction of the secondary. See text for more details.

curves from 10° to 80° . As expected, the wider the emitting region is, the larger the width is. Maximum values of the order of $\text{FWHM} \sim 400 \text{ km s}^{-1}$, as observed, can only be reached for a contribution all along the stream. High K values are obtained for the parts of the stream which are the closest to the white dwarf. Lines formed in the stream at a projected distance from the white dwarf reasonably larger than $0.1 X_L$, the value which corresponds to a typical capture radius at $\sim 21 R_{wd}$, have RV amplitudes restricted to values lower than $\sim 800 \text{ km s}^{-1}$ for a reasonable ($i \leq 70^\circ$) inclination of a non-eclipsing system. For higher white dwarf masses ($1.4 M_\odot$) the curves are shifted up, of the order of 10%, towards greater RV am-

plitudes and widths. The plotted curves are computed for a system of a 3.33h orbital period, but the values do not increase by more than 20% for a typical shorter period of 2h.

These stream properties can be compared with the characteristics of the components that were identified in BY Cam. Narrow components have been found in Balmer lines as well as in the HeII line at different epochs (see Table 2). The properties of the narrow component measured in Feb. 1990 spectra, can be satisfactorily ascribed to the stream but its width value is not much constrained. A large region starting close to the white dwarf and a low inclination angle ($i < 30^\circ$) can account for the measured values. On March 10 1991, the width and the amplitude of the H_β narrow line are compatible with an origin in the stream, for an inclination angle lower than 30° and a large extension of at least $0.1-0.5X_L$ (Fig.7). The data on March 12 are marginally accounted for by an extreme case where the complete stream emits. Alternatively, the fact that this narrow component is mainly visible at phases 0.6-1.0 when its radial velocity passes from red-to-blue may favour instead an origin in the heated face of the secondary (see below).

More interesting is the intermediate width component measured in the HeII line on March 10 1991. Such width is not easily produced on the secondary. It can be produced in the stream for extended regions and high inclinations, but would have rather high velocity amplitudes. The HeII intermediate width component cannot satisfy both requirements (K amplitude and FWHM) for an origin in the stream, the amplitude being much lower than expected from the stream (Fig.7). In addition, its relative phasing with the narrow peak seen in H_β (0.51) is far from the expected value if this last component is indeed formed in the hemisphere of the secondary. In fact, the simulations show that the blue-to-red phasing of the stream component related to the position of the secondary is constrained to an interval of phase of 0.75-0.85 depending on the exact position, where phase zero refers to the inferior conjunction.

On the basis of these simulations of the line emission in the stream, we can also reconsider the possibility that the UV lines arise from such a region, as it has been suggested by Zucker et al. (1995). The mean K radial velocity amplitude of 370 km s^{-1} for CIV and of 245 km s^{-1} for HeII can be easily reproduced with an origin in the stream. The evaluation of the UV line widths is made more difficult in the case of the wide NV, CIV and SiIV doublets which are not resolved with IUE. However, in the case of the HeII 1640 Å line, the blend is made of two very close lines and does not affect the determination. Using archive spectra, the average measured FWHM of the HeII line is of the order of 8 Å. The IUE profiles along the dispersion direction being well represented by gaussian profiles of about

$5.5 \pm 0.3 \text{ \AA}$ FWHM at this wavelength (Cassatella et al. 1985). After deconvolution the intrinsic width of the UV HeII line is then of $\sim 1060 \pm 50 \text{ km s}^{-1}$. The long exposure time may be responsible for part of the broadening. However such a high value is incompatible with the values expected from a stream emission (see Fig. 7), unless the stream is excessively elongated. We note that due to the de-synchronization of the system, the position of the capture radius is in fact modulated at the beat period between the spin and the orbital periods (see Section 6). We have computed this position for given co-latitude angles θ_d of the magnetic field and for different values of the longitudinal angle ψ_d , varying from 0 to 360° , to mimic the variable configuration of the magnetic field. We find that the capture distance r_c varies very little with ψ_d , the strongest modulation (from ~ 21 to $27 R_{wd}$) being found for a high inclined magnetic axis ($\theta_d = 85^\circ$). We obtain a maximum elongated stream for a minimum magnetospheric radius of $\sim 20.6 R_{wd}$, which corresponds to a projected distance on the line of the centres of $\sim 0.1 X_L$. Even an emission from a stream extended down to this value cannot account for the widths of the lines. An alternative origin of the UV lines in the accretion column is proposed in Section 6.

5.2. The heated hemisphere of the secondary

As suggested above, the narrow component seen in the H_β profile in March 1991 might be thought to arise from the X-ray heated hemisphere of the secondary. A lower limit of the white dwarf mass can thus be derived using the radial velocity amplitude of this narrow component. In the case of the extreme hypothesis that the K value represents the motion of the centre of the red dwarf, values of the amplitude K between 200 and 250 km s^{-1} can be obtained for a white dwarf mass $> 0.6 M_\odot$ and an inclination angle i larger than 40° . If, to take into account the decentered position of the gravity centre of the illuminated hemisphere, we apply a K-correction of 1.3, typical value derived from previous studies (Mouchet 1993a), the permitted range of WD masses is then $0.8-1.4 M_\odot$, in agreement with the lower limit found by Ishida et al. (1991), and i should be greater than 50° .

In contrast, for the UV lines, these large widths exclude a dominant origin from the heated secondary. The heated hemisphere has been suggested by Zucker et al. (1995) to contribute some fraction of the NV line. Indeed a narrow component has been clearly detected in the UV lines of AM Her using high resolution spectra (Raymond et al. 1995). It has also been invoked to contribute to the UV HeII line of V1500 Cyg (Schmidt, Liebert & Stockman 1995), but the formation of this line in V1500 Cyg is favoured by the presence of a high temperature white dwarf which strongly contributes to the illumination of the secondary.

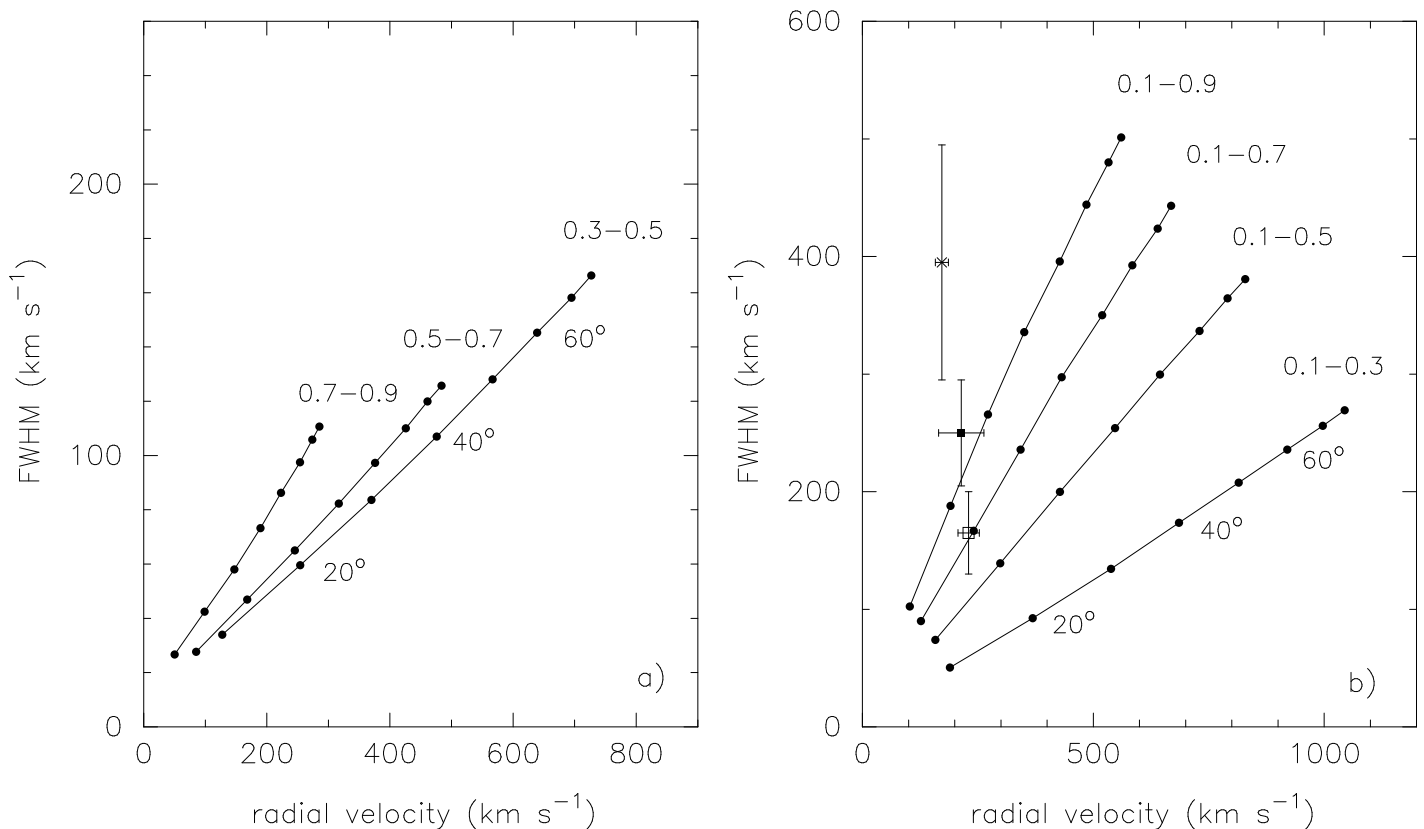


Fig. 7. The orbitally averaged intrinsic FWHM (in km s^{-1}) versus the amplitude of the radial velocity curves for emission lines formed in the ‘horizontal stream’ for different values of the inclination angle (increasing from 10° to 80° along the curves) for two series: at left (a) for a given extension at different positions in the stream; at right (b), for an extension increasing from a region close to the white dwarf. The curves are labeled with the corresponding projected extensions of the emitting region, expressed in units of X_L , the distance between the white dwarf centre and the inner Lagrangian point. The measurements corresponding to the H_β narrow component on March 10 (empty square) and 12 (full square) and to the HeII intermediate width component on March 10 (cross) are also reported.

5.3. Ephemeris: orbital and spin periods

The determination of an exact ephemeris of BY Cam appears to be a tedious task because of the difficulty in defining adequate stable time markers in an asynchronous binary system. Mason et al. (1989) first determined a high accuracy ephemeris based on a recurrent sharp drop in the circular polarization data that was assumed to track correctly the white dwarf rotation. They noted however that their resulting ephemeris was only of apparent high accuracy, given the highly irregular behaviour of the source and the large gaps in their data set. Strictly speaking, this first tentative ephemeris with a period of $(3.322171 \pm 1.4 \cdot 10^{-5} \text{h})$ can therefore only be used as a comparison ephemeris. A possible alias period near 3.351 h was noted by these authors.

The existence of a different longer period ($3.373 \pm 0.007 \text{h}$) was uncovered by SBIOR from an analysis of the H_α narrow line velocity. A similar value was also derived from

the line intensity variations. The narrow line emission is supposed to track the secondary motion and therefore to provide the value of the orbital period. The 1.3% difference with Mason’s period was then interpreted as an evidence of a slight degree of asynchronism of the same type as observed in the classical nova-polar V1500 Cygni (Stockman et al. 1988).

However as more data accumulate, the difference between the two periods becomes less clear. The existence of the longer period was confirmed by more data on the H_α narrow component (Sauter 1992, quoted in Zucker et al. 1995) and recently by the analysis of the UV emission line velocities (Zucker et al. 1995) around a value $(3.3558 \pm 0.0020 \text{h})$, consistent with Sauter’s orbital period. For the shorter period, additional polarimetric data obtained by Pirola et al. (1994) were found to be consistent with a short value $(3.3308196 \pm 3.4 \cdot 10^{-6} \text{h})$, largely outside the error quoted in the initial high accurate ephemeris of MLS. A possible

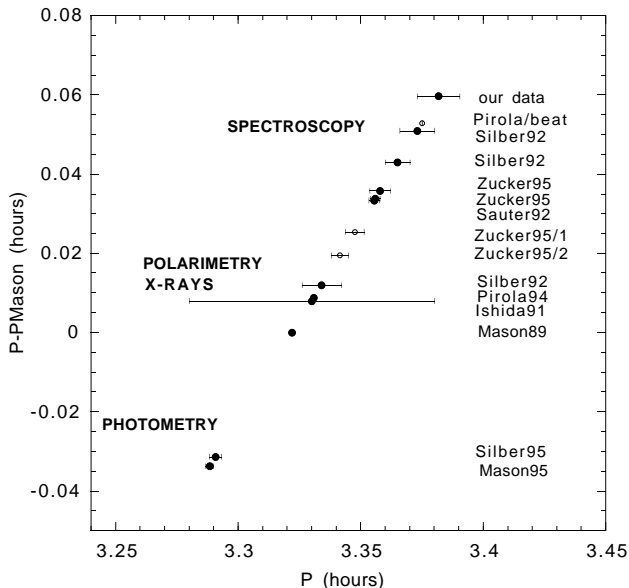


Fig. 8. Schematic representation of the different periods found in BY Cam with the identification of the origin of the data. The open symbols are the different periods determined in this paper. Note the distribution of points according to the nature of data and the nearly continuous distribution.

increase of the photometric/polarimetric period has also been suggested by Pirola et al. and Mason et al. (1995a). More recently, an even shorter period has been reported based on long term photometry by Mason et al. (1995b) and Silber (1995) and has been suggested to be a combination of the spin and the orbital period. Figure 8 shows the different periods presently reported for BY Cam. Ranging from 3.29h to 3.38h, they demonstrate the very confusing situation for this source.

In an attempt to clarify this situation, we have performed a critical re-analysis of existing data, giving particular attention to possible alias periods introduced by the large gaps between different data sets. These gaps cause a loss of the cycle number and prevent the usual (O-C) analysis from being performed. We used a minimization method in which an estimator is computed from the individual timings as :

$$E(P) = \frac{2K}{N(N-1)} \sum_i \sum_{j < i} \frac{[(t_j - t_i)/P]^2}{\sigma_{ij}^2}$$

$$\text{with : } K = \frac{2}{N(N-1)} \sum_i \sum_{j < i} (\sigma_{ij}^2)$$

where P is the trial period, t_i , t_j the individual timings, σ_{ij} the associated errors and N the total number of data points. The K factor is introduced to normalize the

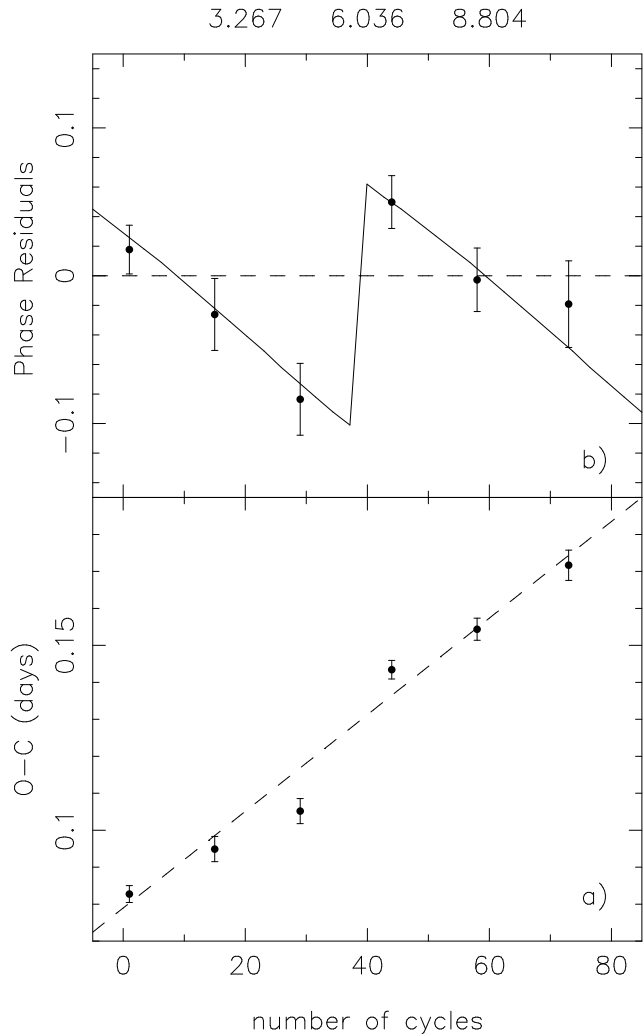


Fig. 9. a): O-C values of the time arrivals for the radial velocity measurements of the UV emission lines given by Zucker et al. (1995). Dotted line is best linear fit. b): Phase residual values after subtraction of the best fit. Note the jump between the third and fourth points. The dot-dashed line represents the prediction from a phase-drift model for a magnetic dipole co-latitude of 12° and a beat period of 14 days (see text).

estimator to the errors. The best period is defined at the estimator minimum. The relevant parameters $(t_j - t_i)/P$ are not independent variables, and thus the estimator does not follow a χ^2 distribution. The statistical significance (*Prob*) was derived from the estimator distribution computed by a Monte Carlo method. We find that this method gives results comparable to the Lomb periodogram (Lomb 1976) but has the advantage of allowing a weighting of the data.

Using this method, we first tried to combine our optical radial velocity narrow line measurements with other measurements (MLS, SBIOR). These four collected data points span nearly five years in total. The best period is

found around 3.38 h, with a 2-day alias at 3.16 h which corresponds to the separation of our last two points, but a number of aliases close to this best value obviously prevents a more accurate determination of the period.

We have also applied this method to the set of data published by Pirola et al. (1994) which gathered timings of the circular polarization dips and of a few photometric broad minima. In the resulting periodogram, the period claimed by Pirola et al. is evident (3.3308 ± 0.0004 h), but another longer period at a similar level of significance ($Prob < 2 \cdot 10^{-5}$) is also present at $3.3749 \pm 4 \cdot 10^{-4}$ h. We note that this last period is consistent with the value derived by SBIOR. A F-test performed to compare the (O-C) residual distributions for the two periods gives no significant difference. The polarimetric data collected over ten years therefore reveal that both the short and long periods coexist in the source. Though at a less significant level, a short beat period at a value of 3.2907 ± 0.0004 h is also present, compatible with the value derived by Silber (1995) and Mason et al. (1995b) from long term photometry (see Section 6).

The discovery of a periodicity in the UV line velocity at a period of 3.3558 h (Zucker et al. 1995), close to the refined 3.3554 h long period value of the narrow H_α velocity reported by Sauter (1992), was unexpected, since it suggests an origin far from the white dwarf for the UV lines. We have reanalysed the data of Table 1 of Zucker et al. (1995). In this case, the accuracy of the data is such that one can keep track of the cycles through the full 11 days of the observations. A standard (O-C) method can therefore be used instead of a periodogram search and provide a more accurate measure of the phase variations inside the observations. We have fitted the NV radial velocity data of the six separate observations with a sine curve at Mason's period (MLS), used as a trial period. The phase residuals (O-C) are plotted in Fig. 9. The evident linear trend clearly confirms that Mason's period does not correctly track the NV velocity. The best period determined from the trend is $P = (3.3535 \pm 0.0029)$ h, in accordance with the value derived by Zucker et al. (1995). However after subtraction of this linear fit, significant residual values are clearly revealed, defining a saw-tooth shape variation through two clearly separated sets of three points. The mid-break corresponds to a phase shift of 0.133. If the two sets of points had been fitted individually, they would have produced two different periods (respectively of 3.3415 ± 0.0035 h and 3.3475 ± 0.0038 h for the first and the second sets), each of them shorter than the mean period derived using all points. The different "alias" periods are shown in Fig. 8, together with all the other period determinations. The period determinations in BY Cam appear roughly distributed in three separate groups depending on the nature of the data with long values derived from spectroscopy, intermediate values from polarimetry and X-rays light curves and short values derived from optical

photometry. But as illustrated by the UV data, there is an apparent continuum of values through the different groups (see discussion in Section 6).

6. Open questions and conclusions

Though it has been extensively observed, the magnetic cataclysmic binary BY Cam is far from been well understood. The debate about the periods has been reactivated by the study of the UV emission lines by Zucker et al. (1995). They demonstrate the presence of the so-called orbital period in the radial velocity measurements of these lines and are led to assume a formation of the UV lines far from the white dwarf, in the orbital plane. We have shown above that, because of their broad widths, the bulk of these lines cannot be produced either in the horizontal stream or in the heated hemisphere. The most natural contribution to the UV lines is the accreting column out of the orbital plane, as it has been previously proposed for several polars, based on the fact that their orbital variations are in phase with the broad optical components (Mukai et al. 1986, de Martino 1995). We show below that the temporal behaviour of the UV lines is indeed consistent with this origin.

The scattering of the periods found in BY Cam (Fig.8) can be explained by a scenario, in which, in the orbital frame, the position of the rotational axis is moving slowly with the beat period of about fourteen days. The accretion column is thus formed along different field lines according to the beat phase. Schematically, the accreted material is slowly dragged by the magnetic field during the relative motion of the white dwarf, up to a certain extent when the accretion is no more possible along these lines. Accretion has then to occur at the opposite pole, causing the jump observed in Fig. 9.

To compute this effect, we have calculated the position, on the white dwarf surface, of the footprints of the field lines which intercept the orbital plane at the capture radius. This is done for a fixed given co-latitude angle θ_d of the dipole magnetic field and for different values of the longitudinal angle ψ_d which measure the different phases inside the beat cycle. When the capture region is close to the white dwarf, the accretion spot is significantly distinct from the magnetic pole and for different capture regions, its location on the white dwarf surface varies. We find that the co-latitude θ_w of the footprint, with respect to the rotational axis, is weakly variable with the beat phase, while its longitude ψ_w , defined in the orbital plane with respect to the line joining the centres of the two stars, may strongly vary along the beat cycle. This implies a lag of the impact spot with respect to the magnetic pole and the resulting phase drift would be interpreted as an apparent period longer than the true spin period.

If furthermore, one assumes that the accretion occurs in the opposite hemisphere as soon as the threading point

is situated at an angular distance from the magnetic axis larger than 90° , then at one time, the computed longitude abruptly goes down to low values and increases again in the cycle. We find that the sudden change of the longitude value, due to the switching of the accretion, occurs before the longitude reaches the standard value of 180° usually expected if one assumes that the accretion occurs at the magnetic pole itself.

In this varying geometry, we have fully computed the phasing of the radial velocity curve produced by material falling down the magnetic lines just above the white dwarf surface. The amplitude of the shift is determined as soon as θ_d and the beat period are fixed. The curve plotted in Figure 9.b) is computed for values of $\theta_d = 12^\circ$ and a beat period of 14 days, and fits the data reasonably well. The RV phase slowly varies with the beat period as observed, distorting the period determination. The sudden change in the phasing when the pole switches, also well reproduces the magnitude of the phase jump ($\sim 50^\circ$) observed in the UV O-C measurements. It appears twice during a beat cycle. A beat value can be evaluated from the point distribution as 14.5 ± 1.5 days. A pole-switching behaviour has been also suggested from photometric data by Silber (1995, Fig.3). However large phase uncertainties are introduced, in this case, by the fact that the shapes of the light curves are variable and strongly depart from a sinusoidal curve.

Strictly speaking, one does not expect to observe the same shape of the beat modulation for lines formed close to the white dwarf and for lines emitted at other positions along the accretion column. The emitting region is also moving, depending on the line production mechanism, and may introduce additional drifts. The present knowledge of the detailed emission line processes at work in these systems is not yet sufficient to allow a better evaluation of this effect.

An interesting consequence of this phase-drift model is the fact that any period determination is biased depending on the length of the observation. Measurements extended on more than a beat period will reveal the orbital period, while data obtained in a few days will show either a shorter period than the orbital one or will not allow any period determination if situated close to the jump. Thus a large spread of period values may result as it is indeed observed in Fig. 8. The considerations above also apply to the broad line components usually thought to be formed in the accretion column. Interestingly, the radial velocities of the H_α broad component measured by Sauter (quoted in Zucker et al. 1995) also show variations at the orbital period (Ω frequency), while they have been found to be modulated with the short spin period (ω frequency) by SBIOR, based on a set of data spread over six nights only. We predict that the O-C measurements by Sauter would mimic the same behaviour as for the NV line.

In addition our reanalysis of Pirola data has shown that a long period is also present in the polarization flux (see

Section 5.3), together with an indication of the $(2\omega - \Omega)$ combination period. These periods are indeed expected for a cyclotron emission produced at the basis of the accretion column (Wynn & King, 1992). By combining the two periods of 3.3308h and 3.3749h found in Pirola polarization data, a short $(2\omega - \Omega)$ period of 3.2878h is derived independently, quite consistent with values determined by Silber (1995) and Mason et al. (1995a,b) from photometric data. From the same two values, a long beat period $(\omega - \Omega)$ of $10.621 \pm 3 \cdot 10^{-3}$ days is also derived. This value is not strictly consistent with the range of values (13-16 days) determined from the UV data, and with the similar 14 day period suggested by Mason et al. (1995a) and Silber (1995).

In conclusion, we have shown that the period determinations are biased depending on the temporal extension of the set of data. The phase-drift model described above explains the inability to determine a unique adequate value for the periods, when the white dwarf is not exactly synchronized. This simple picture has to be modified if one takes into account more physical complex configurations such as a multipole geometry (Mason et al. 1995), a de-centered dipole, field line distortions at the threading region (Hameury, King & Lasota 1986) or possible inhomogeneous blobs in the infalling material. Moreover it is most probable that accretion would occur on both sides for intermediate configurations. The orbital period value is still inaccurate. It can, in principle, be unambiguously established from the study of the absorption lines associated with the companion atmosphere. A search for the Na lines was tentatively done but without success, implying that either the companion is very faint or that it is of an earlier spectral type than had been expected (Zucker et al. 1995). Finally, the discussion of the UV line formation suffers from the absence of a γ -velocity value determination, which combined with the RV amplitude should allow to constrain the emitting region in the accretion column. This can be solved with the Hubble Space Telescope and a higher spectral resolution than provided by the IUE satellite.

Acknowledgments : We are grateful to Didier Pelat for providing us his program SPECTRE and to Paul Mason for useful discussions.

References

- Afanasyev V.L., Lipovetsky V.A., Mikhailov V., Nazarov E., Shapovalova A.I., 1991, *Astrofiz. Issled. (Izv. SAO)*, 31, 128
 Bonnet-Bidaud J.M., Mouchet M., 1987, *A&A* 188, 89
 Bonnet-Bidaud J.M., Mouchet M., Somov N.N., Somova T.A., 1992, in : *Stellar Magnetism*, Eds Yu.V. Glagolevskij, I.I. Romanyuk, p 186
 Bonnet-Bidaud J.M., Mouchet M., Somova T.A., Somov N.N., 1996, *A&A* 306, 199
 Cassatella A., Barbero J., Benvenuti P., 1985, *A&A* 144, 335

- Cropper M., Mason K.O., Allington-Smith J.R., et al., 1989, MNRAS 236, 29P
- Cropper M., 1990, Space Sci. Reviews, 54, 195
- Drabek S.V., Kopylov I.M., Somov N.N., Somova T.A., 1986, Astrofiz. Issled. (Izv. SAO), 22, 64
- Ferrario L., Wickramasinghe D.T., Tuohy, 1989, ApJ 341, 327
- Friedrich S., Staubert, R., Lamer G. et al., 1996, A&A 306, 860
- Hameury J.M., King A.R., Lasota J.P., 1986, A&A 162, 71
- Ishida M., Silber A., Bradt H.V. et al. 1991, ApJ 367, 270
- Ioannisianni B.K., et al., 1982, in : Instrumentation for Astronomy with Large Optical Telescopes, ed. C.M. Humphries, Reidel, p. 3
- Kallman T.R., Schlegel E.M., Serlemitsos P.J., et al., 1993, ApJ 411, 869
- Kaluzny J., Chlebowski T., 1988, ApJ 332, 287
- Katz J.I., 1991, ApJ 374, L59
- Liebert J., Stockman H.S., 1985, in : Cataclysmic Variables and Low Mass X-ray Binaries, eds. D.Q. Lamb & J. Patterson, Reidel, p 151
- Lomb N.R., 1976, Astrophys. and Space Science, 39, 447
- Lubow S., Shu F., 1975, ApJ 198,383
- de Martino D., 1995, in : Proceedings of the Cape Workshop on Magnetic Cataclysmic Variables, eds D.A.H. Buckley and B. Warner, A.S.P. Conf. Ser. Vol. 85, p. 238
- McCarthy P., Bowyer S., Clarke J.T., 1986, ApJ 311, 873
- Mason P.A., Liebert J., Schmidt G.D., 1989, ApJ 346, 941 (MLS)
- Mason P.A., Chanmugam G., Andronov I.L., et al., 1995a, in : Cataclysmic Variables, eds. A.Bianchini, M. Della Valle & M. Orio, Kluwer Academic Publishers, p. 426
- Mason P.A., Andronov I.L., Kolesnikov S.V., Pavlenko E.P., Shakovskoy N.M., 1995b, in : Proceedings of the Cape Workshop on Magnetic Cataclysmic Variables, eds. D.A.H. Buckley and B. Warner, A.S.P. Conf. Ser. Vol. 85, p. 496
- Mouchet M., Bonnet-Bidaud J.M., Hameury J.M., 1991, : 11th North American Workshop on CVs and LMXBs, ed. C.W. Mauche, Cambridge University Press, p 247
- Mouchet M., 1993a, in : Proceedings of the Leicester Meeting on White Dwarfs, ed. M.A. Barstow, Kluwer Academic Publishers, p 411
- Mouchet M., 1993b, in : Proceedings of the Second Haifa Technion Conference: Cataclysmic Variables and Related Physics, Annals of the Israel Physical Society, vol. 10, eds. O. Regev & G. Shaviv, 208
- Mukai K., 1988, MNRAS 232, 175
- Mukai K., Bonnet-Bidaud J.M., Charles P.A., et al. 1986, MNRAS 221, 839
- Neizvestny S.I., 1995, in : Photometric Systems and Standard Stars, ed. Moletai Astronomical Observatory, p. 37
- Pirola V., Coyne G.V., Takalo S.J.L., Larsson S., Vilhu O., 1994, A&A 283, 163
- Raymond J.C., Mauche C.W., Bowyer S., Hurwitz M., 1995, ApJ 440, 331
- Remillard R.A., Bradt H.V., McClintock J.E., Patterson J., 1986, ApJ 302, L11
- Sauter L., 1992, Ph.D. thesis
- Schmidt G.D., Stockman H.S., 1991, ApJ 371, 749
- Schmidt G.D., Liebert J., Stockman H.S., 1995, ApJ 441, 414
- Silber A.D., 1995, in : Proceedings of the Cape Workshop on Magnetic Cataclysmic Variables, eds. D.A.H. Buckley and B. Warner, A.S.P. Conf. Ser. Vol. 85, p. 302
- Silber A., Bradt H.V., Ishida M., Ohashi T., Remillard R.A., 1992, ApJ 389, 704 (SBIOR)
- Somova T. et al., 1982. in : Instrumentation for Astronomy with Large Optical Telescopes, ed. C.M. Humphries, Reidel, p. 283
- Stockman H.S., Schmidt G.D., Lamb D.Q., 1988, ApJ 332, 282
- Vikuliev N., Zinkovskij V., Levitan B., Nazarenko A., Neizvestny S., 1991, Astrofiz. Issled. (Izv. SAO) 33, 158
- Szkody P., Downes R.A., Mateo M., 1990, PASP 102, 1310
- Zucker D.B., Raymond J.C., Silber A.D., et al., 1995, ApJ 449, 310